

Geometrical thermodynamics and P-V criticality of the black holes with power-law Maxwell field

S. H. Hendi^{1,2*}, B. Eslam Panah^{1,2†}, S. Panahiyan^{1,3‡} and M. S. Talezadeh¹

¹ *Physics Department and Biruni Observatory, College of Sciences, Shiraz University, Shiraz 71454, Iran*

² *Research Institute for Astronomy and Astrophysics of Maragha (RIAAM), P.O. Box 55134-441 Maragha, Iran*

³ *Physics Department, Shahid Beheshti University, Tehran 19839, Iran*

We study thermodynamical structure of Einstein black holes in the presence of power Maxwell invariant nonlinear electrodynamics for two different cases. The behavior of temperature and conditions regarding to the stability of these black holes are investigated. Since the language of geometry is an effective method in general relativity, we concentrate on the geometrical thermodynamics to build a phase space for studying thermodynamical properties of these black holes. In addition, taking into account the denominator of heat capacity, we use the proportionality between cosmological constant and thermodynamical pressure to extract the critical values for these black holes. Besides, the effects of variation of different parameters on the thermodynamical structure of these black holes are investigated. Furthermore, some thermodynamical properties such as volume expansion coefficient, speed of sound and isothermal compressibility coefficient are calculated and some remarks regarding these quantities are given.

I. INTRODUCTION

In the early 20th century, it was found that some principal questions could not be resolved by Newton's theory. One of the most notable problems was the prediction of Mercury orbit's orientation. According to these deficits, in 1915 Einstein published a tensorial theory of gravitation which is known as general relativity (GR). GR theory has been accepted as a principal method to define geometrical characteristics of space-time. Black holes and existence of gravitational waves are the most considerable anticipations of GR theory. Recent observations of gravitational waves from a binary black hole merger in LIGO and Virgo collaboration provided a firmly evidence of Einstein's theory [1]. In order to have an effective GR theory, one needs the language of geometry. Hence, the approach one prefers is to concentrate on the technique of geometry without taking into account the complicated algebraic significances.

On the other hand, the coupling of nonlinear sources and GR, attracted significant attentions because of their specific properties. Interesting properties of various nonlinear electrodynamics have been studied before by many authors [2–25]. One of the special classes of the nonlinear electrodynamic sources is power-law Maxwell invariant (PMI), which its Lagrangian is an arbitrary power of Maxwell Lagrangian [26–30]. It is notable that, this Lagrangian is invariant under the conformal transformation $g_{\mu\nu} \rightarrow \Omega^2 g_{\mu\nu}$ and $A_\mu \rightarrow A_\mu$, where $g_{\mu\nu}$ and A_μ are metric tensor and the electromagnetic potential, respectively. This model is considerably richer than Maxwell theory and in a special case (unit power), it reduces to linear Maxwell field (see refs. [26–30], for more details). The studies on the black object solutions coupled to the PMI field have got a lot of attentions in the past decade [31–36].

Another attractive feature of the PMI theory is its conformal invariance, when the power of Maxwell invariant is a quarter of space-time dimensions ($(n+1)/4$, where $(n+1)$ is related to dimensions of space-time). In other words, for the special choice of *power = dimensions/4* ($s = (n+1)/4$, where s is power of PMI), one obtains traceless energy-momentum tensor which leads to conformal invariance. It is notable that the idea is to take advantages of the conformal symmetry to construct the analogues of 4-dimensional Reissner-Nordström solutions with an inverse square electric field in arbitrary dimensions (see refs. [30, 37–40], for more details).

In recent years, more attentions are oriented on the black hole physics, specially its critical behavior and phase transition. Besides, interesting consequences of AdS/CFT correspondence can motivate one for investigating the anti de-sitter space-time. Thermodynamical behavior of the black holes in asymptotically anti de-Sitter space-time was studied first by Hawking and Page [41–44]. Generally, at the critical point where phase transition occurs, discontinuity/divergency of a state space variable such as heat capacity is observed [45].

Recently, the consideration of cosmological constant as a thermodynamical variable, pressure, opened up new avenues in studying black holes. It was possible to obtain van der Waals like behavior and the second order phase transition in thermodynamical phase structure of the black holes. In addition, it was shown that for specific black

* email address: hendi@shirazu.ac.ir

† email address: behzad.eslampanah@gmail.com

‡ email address: sh.panahiyan@gmail.com

holes, reentrant of the phase transition and existence of triple point could be observed [46–69]. The consideration of cosmological constant as a thermodynamical variable has been supported by studies that are conducted in the context of the classical thermodynamics of black holes and gauge/gravity duality [70–74]. One of the methods for obtaining van der Waals like critical points is through the use of heat capacity with a relation between the cosmological constant and pressure [75]. This method has been employed in several papers and it was shown that its results are consistent with those obtained through regular methods.

On the other hand, geometrical thermodynamics (GT), which was first employed by Gibbs and Caratheodory, is another interesting way for investigation of black hole phase transition. Regarding this method, one could build a phase space by employing thermodynamical potential and its corresponding extensive parameters. Meanwhile, divergence points of thermodynamical Ricci scalar provide information related to thermodynamic phase transition points. Historically speaking, first, Weinhold introduced a metric on the equilibrium thermodynamical phase space [76, 77] and after that, it was redefined by Ruppeiner from a different point of view [78, 79]. It is worthwhile to mention that, there is a conformally relationship between Ruppeiner/Weinhold metric. One can obtain that, the conformal factor is inverse of temperature [80]. None of Weinhold and Ruppeiner metrics were invariant under Legendre transformation. The first Legendre invariance metric was introduced by Quevedo [81, 82] which can remove some problems of Weinhold/Ruppeiner methods. Although Quevedo metric can solve some issues of the previous methods, it is confronted with other problems in specific systems. Therefore, in order to remove these problems, a new method was proposed in Ref. [83–86] which is known as HPEM (Hendi-Panahiyan-Eslam Panah-Momennia) metric. In this paper, we want to study thermal stability and phase transition in the context of GT method and extended phase space for black holes in Einstein gravity with the PMI source in higher dimensions. It is notable that in recent years, phase transition, curvatures, Hessian matrix and Nambu brackets have been studied via a new GT method [87–90] which, here, we are not interested to discuss it.

The structure of this paper is as follows. First, we introduce the field equations and black hole solutions in Einstein-PMI gravity. Next, temperature and heat capacity for the obtained black hole solution will be investigated and the stability will be studied. Then, Weinhold, Ruppeiner and Quevedo metrics for studying geometrical thermodynamics of these black holes are employed. It will be seen that, these metrics fail to provide fruitful results. So, we employ the HPEM metric and study the phase transition of these black holes in the context of GT. Next, the critical points are extracted through the use of proportionality between the cosmological constant and pressure. Finally, we finish our paper with some closing remarks.

II. FIELD EQUATIONS AND SOLUTIONS

The action of $(n + 1)$ -dimensional Einstein gravity in the presence of power-law Maxwell field with the negative cosmological constant can be written as

$$I = -\frac{1}{16\pi} \int_M d^{n+1}x \sqrt{-g} [R - 2\Lambda + (-F)^s], \quad (1)$$

where R is the Ricci scalar and s is constant which determining the nonlinearity power of electromagnetic field. The Maxwell invariant $F = F_{\mu\nu}F^{\mu\nu}$, where $F_{\mu\nu}$ is the electromagnetic tensor which is equal to $\partial_\mu A_\nu - \partial_\nu A_\mu$ and A_μ is the gauge potential one-form. One can obtain the field equations by varying action (1) with respect to the gravitational and gauge field, $g_{\mu\nu}$ and A_μ , respectively

$$\begin{aligned} G_{\mu\nu} + \Lambda g_{\mu\nu} &= T_{\mu\nu}, \\ \partial_\mu [\sqrt{-g}(-F)^{s-1} F^{\mu\nu}] &= 0. \end{aligned} \quad (2)$$

In the presence of nonlinear power-law Maxwell invariant field, one can show that the energy-momentum tensor becomes

$$T_{\mu\nu} = \left[\frac{1}{2} g_{\mu\nu} (-F)^s + 2s F_{\mu\sigma} F_\nu^\sigma (-F)^{s-1} \right], \quad (4)$$

and for the case of $s = 1$ Eqs. (2)-(4) reduce to well-known Einstein-Maxwell theory [91]. We apply the following static metric of $(n + 1)$ -dimensional space-time

$$ds^2 = -W(r)dt^2 + \frac{dr^2}{W(r)} + r^2 d\Omega_{n-1}^2, \quad (5)$$

where $W(r)$ is an arbitrary function of radial coordinate which should be determined, and $d\Omega_{n-1}^2$ is the line element of $(n-1)$ -dimensional hypersurface with volume ω_{n-1} which has constant curvature $(n-1)(n-2)k$

$$d\Omega_{n-1}^2 = \begin{cases} d\theta_1^2 + \sum_{i=2}^{n-1} \prod_{j=1}^{i-1} \sin^2 \theta_j d\theta_i^2 & k = 1 \\ d\theta_1^2 + \sinh^2 \theta_1 \left[d\theta_2^2 + \sum_{i=3}^{n-1} \prod_{j=2}^{i-1} \sin^2 \theta_j d\theta_i^2 \right] & k = -1 \\ \sum_{i=1}^{n-1} d\phi_i^2 & k = 0 \end{cases} . \quad (6)$$

Regarding the constant k , one finds that the boundary of $t = \text{constant}$ and $r = \text{constant}$ can be a positive (spherical), negative (hyperbolic) and zero (flat) constant curvature hypersurface. Since we are going to obtain the electrically charged solutions, we consider the consistent gauge potential one-form as $A = h(r)dt$. By considering this radial gauge potential, we find that the Maxwell invariant will be $F = -\left(\frac{dh(r)}{dr}\right)^2$, and therefore, regardless of the values of nonlinearity parameter (s), the solutions are well-defined. Now, taking into account the mentioned gauge potential with Eqs. (2) and (3), one can obtain the metric function as well as the electromagnetic field in following forms [56]

$$W(r) = k - \frac{2\Lambda r^2}{n(n-1)} - \frac{m}{r^{n-2}} + \begin{cases} -\frac{2^{n/2}q^n}{r^{n-2}} \ln\left(\frac{r}{l}\right) & s = \frac{n}{2} \\ \frac{(2s-1)^2 \left(\frac{(n-1)(2s-n)^2 q^2}{(n-2)(2s-1)^2}\right)^s}{r^{2(ns-3s+1)/(2s-1)(n-1)(n-2s)}} & \text{otherwise} \end{cases} , \quad (7)$$

$$F_{tr} = \frac{dh(r)}{dr} = \begin{cases} -\frac{q}{r} & s = \frac{n}{2} \\ -q \left(\frac{2s-n}{2s-1}\right) \sqrt{\frac{(n-1)}{2(n-2)}} r^{-(\frac{n-1}{2s-1})} & \text{otherwise} \end{cases} , \quad (8)$$

where q and m are integration constants which are related to electric charge (Q) and the ADM mass (M) of the black hole in the following manner

$$M = \frac{(n-1)}{16\pi} m, \quad (9)$$

$$Q = \begin{cases} \frac{n}{2\pi} 2^{\frac{n-6}{2}} q^{n-1} & s = \frac{n}{2} \\ \frac{\sqrt{2}(2s-1)s}{8\pi} \left(\frac{n-1}{n-2}\right)^{s-1/2} \left(\frac{(n-2s)q}{2s-1}\right)^{2s-1} & \text{otherwise} \end{cases} . \quad (10)$$

By using the area law, the black hole entropy could be determined as

$$S = \frac{r_+^{n-1}}{4}, \quad (11)$$

where r_+ is the radius of horizon (event horizon). We can also obtain the Hawking temperature of black hole on the outer (event) horizon by using surface gravity interpretation

$$\begin{aligned} T &= \frac{1}{2\pi} \sqrt{-\frac{1}{2}(\nabla_\mu \chi_\nu)(\nabla^\mu \chi^\nu)} = \frac{W'(r_+)}{4\pi} \\ &= \frac{(n-2)k}{4\pi r_+} - \frac{r_+ \Lambda}{2\pi(n-1)} - \begin{cases} \frac{2^{\frac{n-4}{2}} q^n}{\pi r_+^{n-1}} & s = \frac{n}{2} \\ \frac{(2s-1)}{4\pi(n-1)} \frac{\left(\frac{(n-1)(2s-n)^2 q^2}{(n-2)(2s-1)^2}\right)^s}{r_+^{2s(n-2)+1/(2s-1)}} & \text{otherwise} \end{cases} , \end{aligned} \quad (12)$$

where $\chi = \partial_t$ is the Killing vector of the event horizon. Also, the black hole electric potential (U), could be measured at infinity with respect to the event horizon r_+

$$U = \begin{cases} -q \ln\left(\frac{r_+}{l}\right) & s = \frac{n}{2} \\ \sqrt{\frac{(n-1)}{2(n-2)}} \frac{q}{r_+^{(n-2s)/(2s-1)}} & \text{otherwise} \end{cases} . \quad (13)$$

It is straightforward to show that these quantities satisfy the first law of thermodynamics,

$$dM = TdS + UdQ. \quad (14)$$

The case where $s = \frac{n}{2}$ is known as conformally invariant Maxwell (CIM). Through the paper, we will divide the solutions to the cases of CIM (where $s = \frac{n}{2}$) and PMI ($s \neq \frac{n}{2}$) solutions. In the following, by using the geometrical thermodynamics approach, we want to study the phase transitions of black hole.

III. THERMODYNAMICAL STRUCTURE

A. Temperature

1. PMI case

In the case of PMI, it is evident that signature of the temperature depends on choices of different parameters. Here, for the AdS spherical case, the topological (κ) and cosmological constant (Λ) terms are contributing to positivity of the temperature. Interestingly for the charge term, depending on choices of nonlinearity parameter, s , this term may contribute to the negativity or positivity of temperature. For $s > 1/2$, the charge term will always have negative effect on the temperature while for violation of this condition, it will have a positive contribution. It is crucial to mention that this dual behavior is due to contribution of the generalization to nonlinear electromagnetic field. In other words, by setting $s = 1$, the charge term will only have negative effect on the temperature (contribution to positivity does not exist). This highlights the effects of nonlinear electromagnetic field on the thermodynamical structure of black holes. That being said, one can point out that for violation of the mentioned condition, for spherically symmetric AdS black holes, temperature will be positive without any root.

For small values of the horizon radius, dominant term is the charge term while for the large values of horizon radius, Λ term will be dominant. For spherically symmetric AdS space-time, Λ term is positive. Therefore, for the large values of horizon radius, temperature will be positive. Therefore, there exists a root for the temperature, r_0 , in which for $r_+ < r_0$, the temperature is negative and solutions are not physical.

On the contrary, due to negative contribution of the Λ in spherical dS space-time, the temperature will be negative for large values of horizon radius. The effective term here is topological term. In other words, by suitable choices of different parameters, for a region of horizon radius, topological term would be dominant which results into formation of an extremum (maximum) and existence of two roots. Between these two roots, temperature is positive and solutions are physical (otherwise, temperature is negative). It is worthwhile to mention that for hyperbolic horizon, the temperature will be always negative in this case. Therefore, there is no any physical solution in this case.

Now, we focus on effects of each parameter on negativity/positivity of the temperature. Evidently, by increasing dimensions, the effect of topological and charge terms increase while the opposite takes place for Λ . As for nonlinearity parameter, for $r_+ > 1$, if $0.5 < s < 1$, then the effects of charge term is an increasing function of s , while if $1 < s$, the effects of charge term will be a decreasing function of s . It is worthwhile to mention that for $r_+ < 1$, for both cases of $0.5 < s < 1$ and $1 < s$, the charge term is a decreasing function of the nonlinearity parameter. We should point it out that we have excluded $s = 1$, since it is Maxwell case. In addition, the effect of charge term is an increasing function of the electric charge. Now, by considering mentioned effects, one is able to determine the thermodynamical behavior of these black holes in the context of temperature and study different limits which these black holes have.

2. CIM case

In the CIM case, contribution of the charged term is always toward negativity of the temperature. The dominant term for the small values of horizon radius is the charge term which is negative. For the medium and large values of horizon radius, the dominant terms, respectively, are topological and Λ terms. Considering the dominance of different terms, depending on choices of topology and type of space-time, the temperature could be one of the following cases:

I) For dS space-time and $k = 0, -1$, all the terms in temperature are negative. Therefore, temperature will be negative and solutions are not physical.

II) For dS space-time and $k = 1$, only the topological term is positive whereas the charge and Λ are negative. Remembering that for small and large black holes, the dominant term are q and Λ terms, it is possible to find two roots for temperature and one maximum which is located at the positive values of temperature. This leads to presence of physical solutions only for medium black holes while for large and small black holes, physical black holes are absent.

III) For AdS space-time, the Λ term has positive contribution. Remembering that for small and large black holes, dominant terms are q and Λ terms, respectively, irrespective of topological structure of the black holes, there exists a root for the temperature. For black holes smaller than this root, temperature is negative and solutions are non-physical. For $k = 0, -1$, the temperature is only an increasing function of the horizon radius. Whereas, by suitable choices of different parameters, in case of $k = 1$, temperature may acquire one or two extrema. The behavior of temperature in this case is similar to $T - r_+$ diagrams in extended phase space (similar ones in van der Waals like black holes), which indicates that a second order phase transition takes place for these black holes. It is worthwhile to mention that extrema in temperature are matched with divergencies in the heat capacity which results into the existence of second order phase transition in thermodynamical structure of the black holes.

B. Heat capacity and stability

Next, we study the stability conditions of these black holes. To do so, we employ the canonical ensemble which is based on the heat capacity. The stability conditions are determined by the behavior of heat capacity. In other words, the sign of heat capacity represents thermal stability/instability of the system. The positivity indicates that system under consideration is in thermally stable state. In addition, there are two types of points which could be extracted by using the heat capacity: bound and phase transition points. The bound point is where the heat capacity (temperature) acquires a root. The reason for calling it bound point comes from the fact that it is where the sign of temperature is changed. Since the negative temperature is representing a non-physical solution, this point marks a bound point. On the other hand, phase transition point is where a discontinuity exists for the heat capacity.

The heat capacity is given by

$$C_Q = \frac{\left(\frac{\partial M}{\partial S}\right)_Q}{\left(\frac{\partial^2 M}{\partial S^2}\right)_Q} = T \left(\frac{\partial S}{\partial T}\right)_Q, \quad (15)$$

where by employing Eqs. (11) and (12), one can find

$$C_Q = \begin{cases} -\frac{(n-1)(n-2)kr_+^{2n-3} - 2\Lambda r_+^{2n-1} - 2^{\frac{n}{2}}(n-1)q^n r_+^{n-1}}{4\left[(n-2)kr_+^{n-2} + \frac{2\Lambda}{(n-1)}r_+^n - 2^{\frac{n}{2}}(n-1)q^n\right]} & s = \frac{n}{2} \\ -\frac{(n-1)(n-2)kr_+^{\frac{4ns-n+2}{2s-1}} - 2\Lambda r_+^{\frac{4s(n+1)-n}{2s-1}} - (2s-1)\left(\frac{(n-1)(n-2s)^2 q^2}{(n-2)(2s-1)^2}\right)^s r_+^{\frac{6s+n(2s-1)}{2s-1}}}{4\left[\frac{2(n+1)}{(n-2)kr_+^{\frac{2(n+1)}{2s-1}} + \frac{2\Lambda}{(n-1)}r_+^{\frac{2s(n+2)}{2s-1}} - \frac{(2s(n-2)+1)}{(n-1)}\left(\frac{(n-1)(n-2s)^2 q^2}{(n-2)(2s-1)^2}\right)^s r_+^{\frac{6s}{2s-1}}\right]} r_+ & otherwise \end{cases}. \quad (16)$$

1. PMI case

The positivity of heat capacity is determined by the signature of denominator and numerator of it. Here, in order to have a positive heat capacity, two different cases could be considered; whether numerator (A) and denominator (B) are positive or both of them are negative ($A \times B > 0$);

$$A = 2\Lambda r_+^{\frac{4s(n+1)-n}{2s-1}} + (2s-1) \left(\frac{(n-1)(n-2s)^2 q^2}{(n-2)(2s-1)^2}\right)^s r_+^{\frac{6s+n(2s-1)}{2s-1}} - (n-1)(n-2)kr_+^{\frac{n(4s-1)+2}{2s-1}},$$

$$B = (n-2)kr_+^{\frac{2(n+1)}{2s-1}} + \frac{2\Lambda}{(n-1)}r_+^{\frac{2s(n+2)}{2s-1}} - \frac{(2s(n-2)+1)}{(n-1)} \left(\frac{(n-1)(n-2s)^2 q^2}{(n-2)(2s-1)^2}\right)^s r_+^{\frac{6s}{2s-1}}.$$

Therefore, two set of conditions should be satisfied to have a positive heat capacity, hence, thermally stable solutions. Due to complexity of the obtained heat capacity for PMI case, it is not possible to extract bound and phase transition points analytically. Therefore, we employ numerical approach to study stability and obtain bound and phase transition points of these black holes. The results of numerical evaluation is presented in following diagrams (Figs. 1-3).

Depending on the choices of different parameters, for AdS space-time, the temperature could be only an increasing function of the horizon radius with one root (right panel of Fig. 1 and left panels of Figs. 2 and 3) or it may acquire extrema with one root (left and middle panels of Fig. 1; middle and right panels of Figs. 2 and 3). The temperature and heat capacity share same root. This is the bound point. For $r_+ < r_0$ (r_0 is the root), solutions have negative temperature and heat capacity. Therefore, in this region, solutions are non-physical ones.

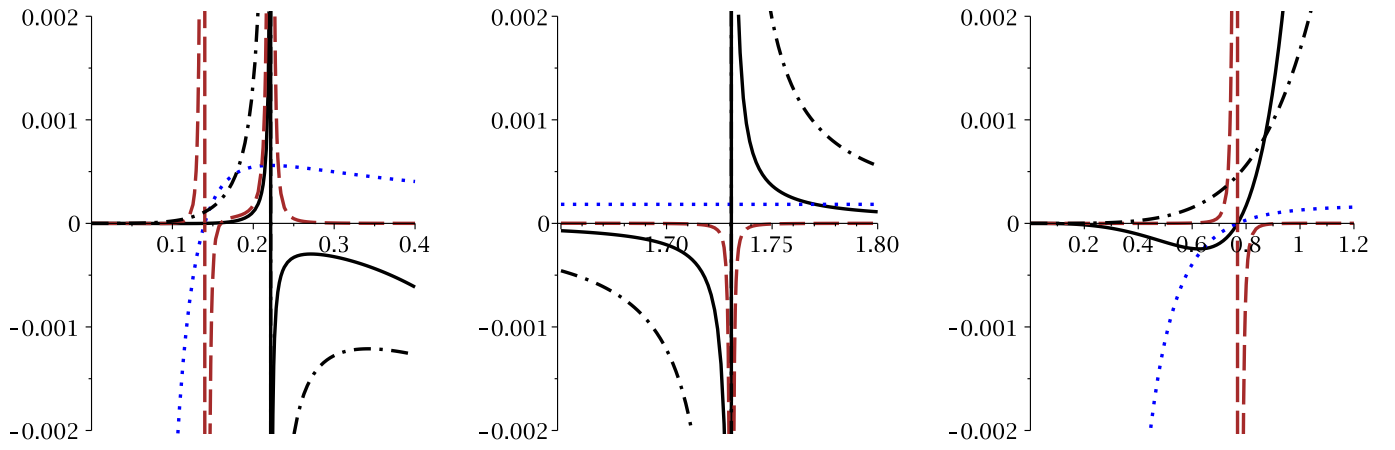


FIG. 1: **HPEM metric:** \mathcal{R} (dashed line), T (dotted line), α (dashed-dotted line) and C_Q (continues line) versus r_+ for $\Lambda = -1$, $s = 1.2$ and $n = 4$; Left and middle panels: $q = 0.1$, right panel: $q = 1$ (For different scales).

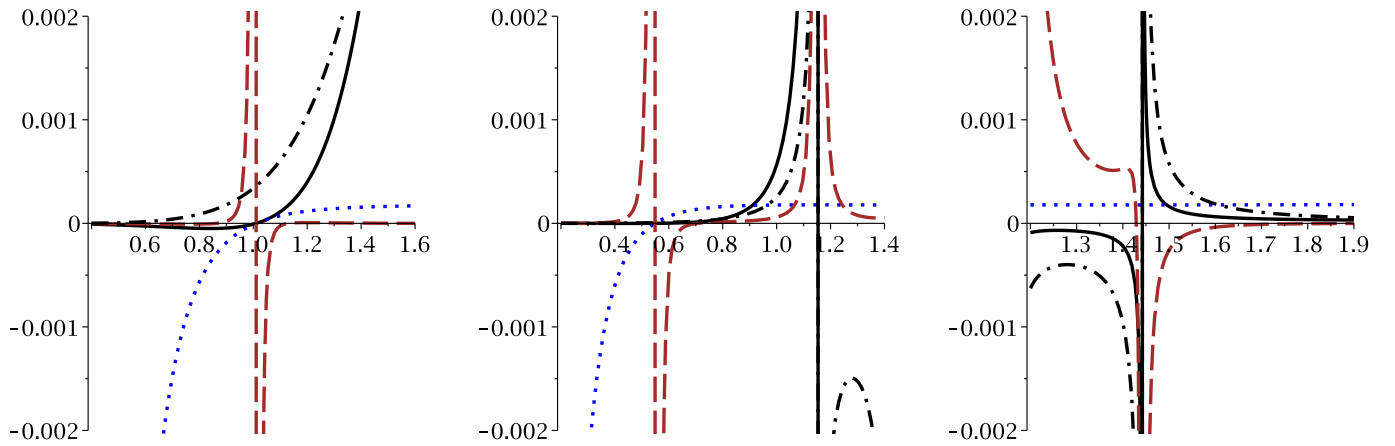


FIG. 2: **HPEM metric:** \mathcal{R} (dashed line), T (dotted line), α (dashed-dotted line) and C_Q (continues line) versus r_+ for $\Lambda = -1$, $q = 1.1$ and $n = 4$; Left panel: $s = 0.9$, middle and right panels: $s = 1.4$ (For different scales).

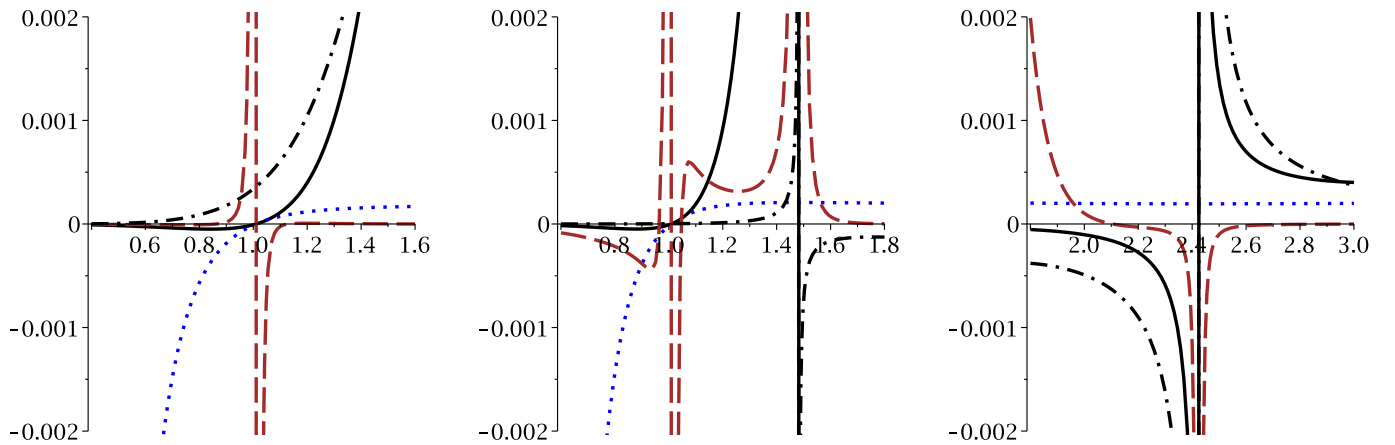


FIG. 3: **HPEM metric:** \mathcal{R} (dashed line), T (dotted line), α (dashed-dotted line) and C_Q (continues line) versus r_+ for $\Lambda = -1$, $q = 1.1$ and $s = 1.2$; Left panel: $n = 4$, middle and right panels: $n = 5$ (For different scales).

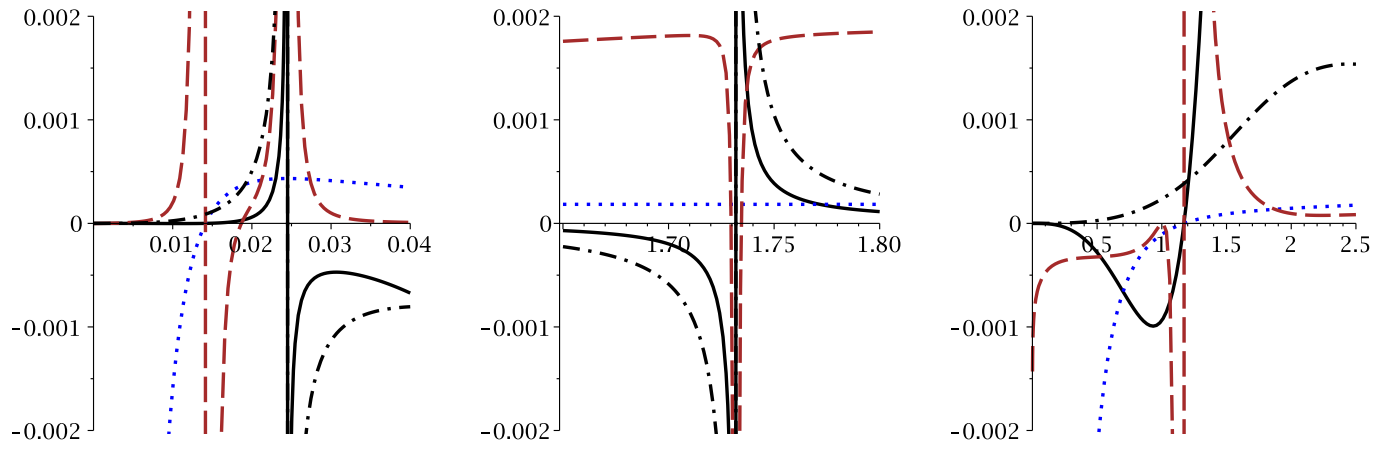


FIG. 4: **HPEM metric:** \mathcal{R} (dashed line), T (dotted line), α (dashed-dotted line) and C_Q (continues line) versus r_+ for $\Lambda = -1$, $l = 1$ and $n = 4$; Left and middle panels: $q = 0.1$, right panel: $q = 1$ (For different scales).

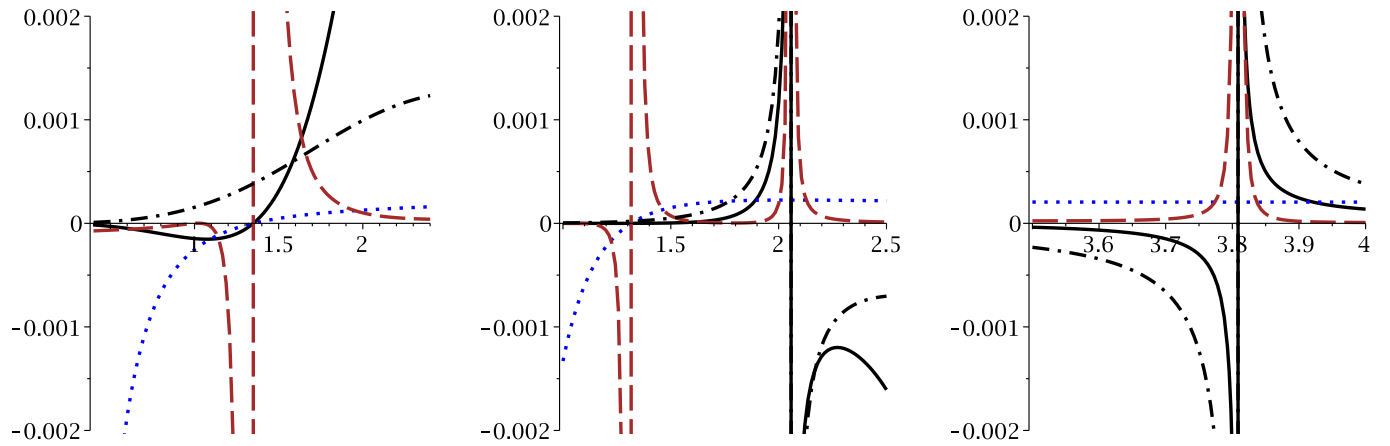


FIG. 5: **HPEM metric:** \mathcal{R} (dashed line), T (dotted line), α (dashed-dotted line) and C_Q (continues line) versus r_+ for $\Lambda = -1$, $q = 1.1$ and $l = 1$; Left panel: $n = 4$, middle and right panels: $n = 7$ (For different scales).

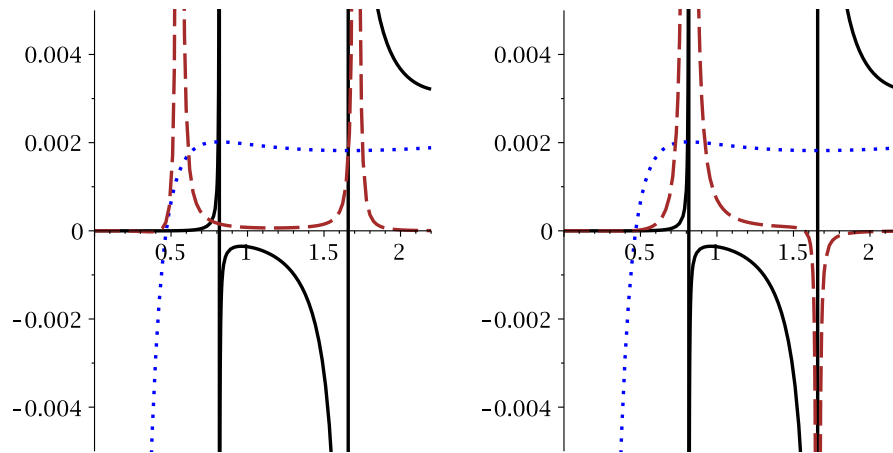


FIG. 6: \mathcal{R} (dashed line), T (dotted line) and C_Q (continues line) versus r_+ for $\Lambda = -1$, $s = 1.2$, $q = 0.5$ and $n = 4$; Left: Weinhold metric, right panel: Quevedo metric (For different scales).

For small values of q , the temperature will have two extrema. In places of these extrema, heat capacity is divergent (left and middle panels of Fig. 1). In other words, in places of these extrema, system goes under second order phase transitions. By increasing electric charge, these extrema are vanished and only a bound point will remain (right panel of Fig. 1). As for nonlinearity parameter, its effects are opposite of those of electric charge. In other words, by increasing nonlinearity parameter, the extrema for temperature and divergencies for heat capacity are formed (middle and right panels of Fig. 2) while for small values of this parameter, only bound point is observed (left panel of Fig. 2). The effects of dimensionality are similar to those observed for nonlinearity parameter. Meaning that by increasing dimensionality, two extrema are formed and system will acquire second order phase transitions in its phase space in higher dimensions (Fig. 3).

As for stability, if only bound point is observed, physical stable solutions is observed only for $r_0 < r_+$. The formation of extrema modifies the stability conditions of these black holes. In this case, bound point and two divergencies of the heat capacity determine stable regions and phase transitions. Between bound point and smaller divergence point, both temperature and heat capacity are positive. Therefore, the solutions are physical and stable in this region. On the other hand, between two divergencies, temperature is positive while heat capacity is negative, which leads to solutions being physical and unstable. Finally after larger divergence, both heat capacity and temperature are positive and solutions are stable. Thermodynamical concepts indicate that system in unstable state goes under phase transition and acquires stability. By taking this matter into account, in smaller divergence a phase transition of larger to smaller takes place while vice versa happens in larger divergence.

2. CIM case

First, lets study the conditions for the positivity/negativity of the solutions. In order to have positive heat capacity, it needs to satisfy $A' \times B' > 0$ in which

$$A' = 2\Lambda r_+^{2n-1} + 2^{\frac{n}{2}}(n-1)q^n r_+^{n-1} - (n-1)(n-2)kr_+^{2n-3},$$

$$B' = (n-2)kr_+^{n-2} + \frac{2\Lambda}{(n-1)}r_+^n - 2^{\frac{n}{2}}(n-1)q^n,$$

where A' and B' are, respectively, the numerator and the denominator of heat capacity.

It is not possible to obtain roots and divergencies of the heat capacity for this case, analytically. Therefore, we employ numerical methods and plot following diagrams for studying the effects of different parameters (Figs. 4 and 5).

It is evident that for small q , temperature has one root with two extrema. The roots of temperature and heat capacity coincide with each other while the extrema of temperature are matched with divergencies of the heat capacity. These divergencies are phase transition points. Increasing the electric charge leads to elimination of phase transition points while there exists a root for temperature and heat capacity (see Fig. 4 for more details). The opposite behavior is observed for the effects of dimensionality. Meaning that by increasing dimensionality, system with one bound point, acquires one root and two divergencies. In other words, by increasing dimensions, the thermodynamical structure of the black holes is modified and black holes will enjoy second order phase transition in their phase diagrams (Fig. 5).

C. Geometrical thermodynamics

Regarding ordinary laboratory systems (short-range interaction property; entropy is proportional to volume), it is expected to obtain the same thermodynamic properties for all ensembles. However, taking into account the holography conception, one finds that black holes are not ordinary systems (long-range interaction property; entropy is proportional to area) [94–100]. Therefore, one may obtain different results in the context of various ensembles of black hole thermodynamics [101]. Regardless of tracing ensemble dependency, it was shown that there are some extra poles (or mismatch with other methods) in the Ricci scalar of Weinhold, Ruppeiner and Quevedo metrics. Existence of these anomalies/mismatches motivate one to build another Legendre invariant thermodynamic metric which can be conformally related to Quevedo metric. HPEM metric is the same as Quevedo metric up to a conformal factor. Since the differences in the conformal factor comes from the mass and its derivatives, it is expected that HPEM enjoys Legendre invariancy, but with a different Legendre multiplier. It is also worthwhile to mention that the Legendre invariance alone is not sufficient to guarantee a unique picture of thermodynamical metrics in terms of their curvatures [102]. In other words, in addition to Legendre invariancy, we need to demand curvature invariancy under a change

of representation. As a result, it will be worthwhile to consider the investigation of both Legendre and curvature invariances.

Here, we will employ the geometrical thermodynamics to study both bound and phase transition points of these black holes. The geometrical thermodynamics is based on constructing phase space by using one of the thermodynamical quantities as thermodynamical potential. The information regarding bound and phase transition points are stored in Ricci scalar of this phase space. In other words, the divergencies of this Ricci scalar present bound and phase transition points. (For more details regarding the meaning of curvature scalar in geometrical thermodynamics, we refer the reader to Ref. [92]). Depending on choice of thermodynamical potential, the components of phase space differ (this is due to fact that each thermodynamical quantity has its specific extensive parameters). There are several well known methods for constructing phase space; Weinhold [76, 77], Ruppeiner [78, 79], Quevedo [81, 82] and HPEM [83–86]. In order to investigate thermodynamical properties of the system, the successful method has divergencies which exactly are matched with bound and phase transition points. The mentioned well-known thermodynamical metrics in the context of geometrical thermodynamics are given by

$$ds^2 = \begin{cases} M g_{ab}^W dX^a dX^b & \text{Weinhold} \\ -T^{-1} M g_{ab}^R dX^a dX^b & \text{Ruppeiner} \\ (SM_S + QM_Q) (-M_{SS} dS^2 + M_{QQ} dQ^2) & \text{Quevedo} \\ S \frac{M_S}{M_{QQ}^3} (-M_{SS} dS^2 + M_{QQ} dQ^2) & \text{HPEM} \end{cases}, \quad (17)$$

in which $M_X = \partial M / \partial X$ and $M_{XX} = \partial^2 M / \partial X^2$. The denominators of their Ricci scalars will be [83]

$$\text{denom}(\mathcal{R}) = \begin{cases} M^2 (M_{SS} M_{QQ} - M_{SQ}^2)^2 & \text{Weinhold} \\ M^2 T (M_{SS} M_{QQ} - M_{SQ}^2)^2 & \text{Ruppeiner} \\ M_{SS}^2 M_{QQ}^2 (SM_S + QM_Q)^3 & \text{Quevedo} \\ 2S^3 M_{SS}^2 M_S^3 & \text{HPEM} \end{cases}. \quad (18)$$

It is worthwhile to mention that Weinhold and Ruppeiner metrics were formally introduced as the Hessian of the internal energy (mass) and entropy, respectively

$$ds^2 = \begin{cases} \frac{\partial^2 M}{\partial X^a \partial X^b} dX^a dX^b & \text{Weinhold} \\ -\frac{\partial^2 S}{\partial X^a \partial X^b} dX^a dX^b & \text{Ruppeiner} \end{cases}. \quad (19)$$

Later, it was shown that these two methods are conformally related by adding terms which could be seen in Eq. (17). In this paper, we employ the forms which are given in Eq. (17) for Weinhold and Ruppeiner methods.

Before we continue our study, it is worthwhile to point out a few remarks regarding HPEM metric. The HPEM and Quevedo metrics have similar structure up to a conformal factor with same signature which is $(-+++ \dots)$. In Ref. [93], it was shown that it is possible to obtain an infinite number of Legendre invariant metrics. The simplest way to construct Legendre invariant metrics is to apply a conformal transformation. Considering the similar structure of HPEM and Quevedo metrics with same signature, it is expected that with a different Legendre multiplier, HPEM also enjoys Legendre invariance. The studies conducted in the context of HPEM metric showed that signature of the curvature scalar of this metric around divergencies provides the possibility to recognizing the type of phase transition (smaller to larger or vice versa). In addition, by studying signature, it is possible to differ bound and phase transition points from one another. These differences in signature around divergencies also enables one to have a picture regarding stability/instability of black holes. One of the main properties of this metric is to include bound points in its divergencies. This results into having a better and more complete picture regarding thermodynamical structure of the black holes comparing to previous metrics. In addition, it was shown that the results of this metric is in agreement with other methods of studying thermodynamical structure of the black holes such as the heat capacity, van der Waals like diagrams and etc [75, 103, 104].

Existence of M_S and M_{SS} in denominator of the HPEM metric ensures that bound and phase transition points are matched with divergencies of the Ricci scalar without any extra divergency. As for Quevedo metric, since M_{SS} is

present in denominator of this metric, phase transition points are matched with divergencies of the Ricci scalar. On the other hand, the bound points are matched only when

$$M_S = -\frac{QM_Q}{S}, \quad (20)$$

which in general is not satisfied. In addition, the presence of M_{QQ} may lead to existence of extra divergencies which are not matched with bound and phase transition points. Such a case has been reported for several black holes before [83–86]. Analytical evaluation shows that M_{QQ} for these black holes will not lead to any extra divergency, but $M_S = -\frac{QM_Q}{S}$ is not satisfied.

Recently, in Ref. [105], it was pointed out that Quevedo metric should have the following form instead of the one pointed out in Eq. (17),

$$ds^2 = M (-M_{SS}dS^2 + M_{QQ}dQ^2), \quad (21)$$

where the denominator of its Ricci scalar will be

$$denom(\mathcal{R}) = M^3 M_{SS}^2 M_{QQ}^2. \quad (22)$$

Here, the condition which was observed for the previous case (20) is eliminated for the Ricci scalar. The divergencies of heat capacity are included through the presence of M_{SS}^2 term. Meanwhile, the existence of M_{QQ} results into presence of divergencies for Ricci scalar which are not consistent with any phase transition point. Recently, through several studies it was shown that it is possible for the mass of the black holes to have root(s) [106, 107]. This indicates that for this form of the Quevedo metric, the existence of M and its roots may provide the possibility of the existence of divergencies in its Ricci scalar which are not matched with any phase transition point. Therefore, cases of mismatch between divergencies of the Ricci scalar of this Quevedo metric and phase transition points are possible. It is worthwhile to mention that this case of Quevedo metric does not include bound points in divergencies of its Ricci scalar.

In case of Weinhold and Ruppeiner, it was not analytically possible to see whether divergencies of Ricci scalars of these methods coincide completely with bound and phase transition points. Therefore, we employed numerical methods and plotted some diagrams (see Fig. 6).

Evidently, employing Weinhold and Quevedo metrics will lead to inconsistent results regarding bound and phase transition points. In other words, by taking a closer look at the plotted diagrams (see Fig. 6), it is obvious that there is a mismatch between divergencies of Ricci scalar of Weinhold metric and bound and phase transition points. In addition, the Quevedo metrics fails to produce divergency in its Ricci scalar which is coincidence with bound point. On the contrary, divergencies of the Ricci scalar of HPEM metric coincide with the bound and phase transition points completely (see Figs. 1-5).

One of the interesting properties of HPEM metric is the behavior of its Ricci scalar around bound and phase transition points. If the divergency is related to the phase transition of larger to smaller black holes, the signature of Ricci scalar around it, is positive. On the contrary, for phase transition of smaller to larger black holes, the sign of Ricci scalar around this divergence point is negative. As for the bound point, interestingly, the signature of Ricci scalar changes around this divergence point. These changes in the signature of Ricci scalar enable one to recognize the type of points without prior knowledge about heat capacity. As for Ruppeiner, since it has conformal relation with Weinhold metric, same results are applicable for phase transition points. But, due to the existence of temperature in denominator of Ricci scalar of Ruppeiner, the bound points are matched with some of the divergencies.

To summarize, we saw that employing Weinhold, Ruppeiner and Quevedo metrics, leads to the existence of divergencies in the Ricci scalar which are not match with the obtained bound and phase transitions of heat capacity, while the HPEM metric provides a consistent number of divergencies in the places of bound and phase transition points. Furthermore, the characteristic behavior of Ricci scalar of HPEM metric enables one to recognize the type of point and phase transition.

D. Critical behavior in extended phase space

In this section, we will conduct a study regarding possible existence of critical and van der Waals like behavior for the solutions. Recently, there has been a novel interpretation for the cosmological constant in AdS black holes. Instead of considering this parameter as a fixed one, it was proposed to consider it as a thermodynamical variable. By doing so, the thermodynamical structure of black holes is enriched and it is possible to introduce new phenomenologies such as van der Waals like behavior and phase transition for black holes. The van der Waals like behavior of these black

holes through usual method was investigated in Ref. [56]. Here, we would like to study critical values through a new method which was introduced in Ref. [75]. In this method, the cosmological constant is replaced by its proportional pressure in the heat capacity. Then, by using denominator of the heat capacity and solving it with respect to the pressure, a relation for pressure is obtained which is different from the usual equation of state. The maximum of this relation marks a place in which phase transition takes place. In other words, the maximum of this relation in $P - r_+$ diagram is corresponding to the critical pressure. This method was employed in several papers and it was shown to have consistent results with those extracted through usual methods [75, 103, 104].

The proportionality between cosmological constant and pressure is given by

$$P = -\frac{\Lambda}{8\pi}. \quad (23)$$

By replacing the cosmological constant with its corresponding thermodynamical pressure, the mass of black holes will play the role of enthalpy instead of internal energy. Using this new concept for the mass of black holes, it is a matter of calculation to obtain the volume of black holes, conjugate to the thermodynamical pressure, in following form

$$V = \left(\frac{\partial H}{\partial P} \right) = \left(\frac{\partial M}{\partial P} \right) = \frac{r_+^{n-2}}{n-2}. \quad (24)$$

Evidently, the volume is a smooth function of the horizon radius and it is only horizon radius and dimension dependent. This relation between the horizon radius and volume provides the possibility of employing horizon radius instead of volume to study phase diagrams of the black holes. In other words, the horizon radii in which system goes under phase transition could be used to obtain critical volume of our thermodynamical systems.

Now, by using the heat capacity (16) with (23) and solving the denominator of heat capacity with respect to thermodynamical pressure, one obtains the following relation for pressure

$$P = \begin{cases} \frac{(n-1)}{16\pi r_+^n} [(n-2)kr_+^{n-2} - 2^{\frac{n}{2}}(n-1)q^n] & s = \frac{n}{2} \\ \frac{(2(2-n)s-1) \left[\frac{(n-1)(n-2s)^2 q^2}{(n-2)(2s-1)^2} \right]^s r_+^{\frac{6s}{2s-1}} + k(n-1)(n-2)r_+^{\frac{2(ns+1)}{2s-1}}}{16\pi r_+^{\frac{2s(n+2)}{2s-1}}} & otherwise \end{cases}. \quad (25)$$

Using this relation, we are in a position to study possible existence of phase transition for these black holes. Obtained relation for pressure consists two terms; charge term and topological term. The charge term has always negative contribution to pressure. Therefore, the existence of critical behavior is determined by the topological term. That being said, one can automatically conclude that for $k = 0, -1$, no critical behavior exists. In other words, for these two cases, the pressure will be negative which indicates that no critical behavior is observed. Regarding the fact that maximum of the pressure (25) is where second order phase transition takes place, one can, analytically, show that the maximum of this pressure is located at the following horizon radius

$$r_{critical/\max} = \begin{cases} \left(\frac{2^{\frac{(n-2)}{2}} n(n-1)q^n}{k(n-2)} \right)^{\frac{1}{n-2}} & s = \frac{n}{2} \\ \left(\frac{2s^2(n-2)+s}{k(n-2)(2s-1)} \right)^{\frac{2s-1}{s(n-3)+1}} \left(\frac{(n-1)(n-2s)^2 q^2}{(n-2)(2s-1)^2} \right)^{\frac{s(2s-1)}{s(n-3)+1}} & otherwise \end{cases}, \quad (26)$$

where by replacing the horizon radius, one finds

$$P_{critical/\max} = \begin{cases} \frac{k(n-1)(n-2)^2}{16n\pi} \left(\frac{2^{\frac{(n-2)}{2}} n(n-1)q^n}{k(n-2)} \right)^{\frac{2}{2-n}} & s = \frac{n}{2} \\ \frac{\frac{s(n+1)-1}{k s(n-3)+1} \Upsilon}{16\pi(2s-1)^{\frac{2-8s^2}{1+(n-3)s}}} \left(1 - \frac{2k \left[\frac{(n-2)(2s-1)^2}{(n-1)} \right]^{\frac{(n-3)s^2+(n-2)s+1}{s(n-3)+1}}}{s^2[2s(n-2)+1][q^2(n-2s)^2]^s} \right) & otherwise \end{cases}, \quad (27)$$

in which

$$\Upsilon = \frac{(n-2)^{\frac{4s^2+s(n-1)-1}{1+(n-3)s}} (n-1)^{\frac{1-4s^2+s(n-1)}{1+(n-3)s}}}{\{q^{2s}(n-2s)^{2s} [1+2s(n-2)] s\}^{\frac{2(2s-1)}{1+(n-3)s}}}.$$

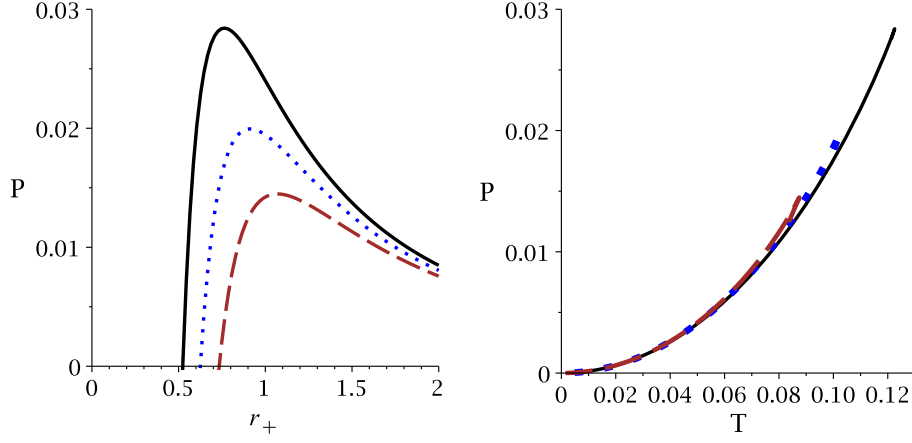


FIG. 7: Left panel: P versus r_+ diagrams; Right panel: P versus T diagrams. for $k = 1$, $n = 3$ and $s = 1.2$; $q = 0.9$ (continues line), $q = 1$ (dashed line) and $q = 1.1$ (dotted line).

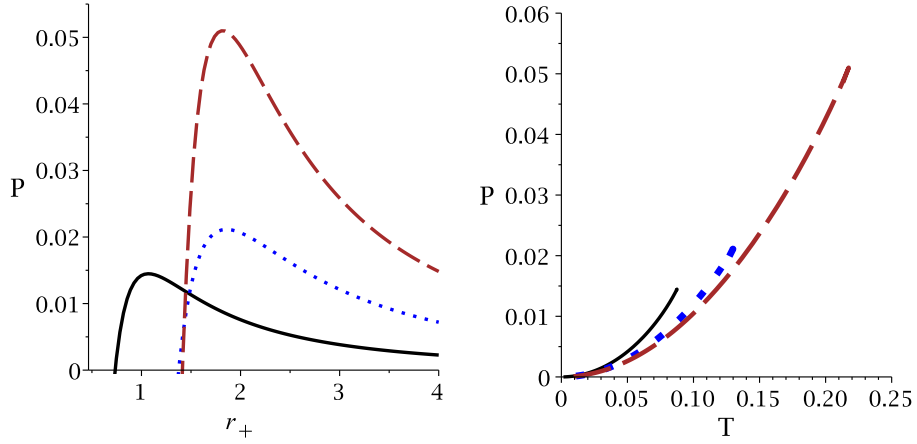


FIG. 8: Left panel: P versus r_+ diagrams; Right panel: P versus T diagrams. for $k = 1$, $s = 1.2$ and $q = 1.1$; $n = 3$ (continues line), $n = 4$ (dashed line) and $n = 5$ (dotted line).

Obtained relation for the critical pressure indicates that the positivity of critical pressure is subject to variation of different parameters. It is evident that for Ricci-flat horizon ($k = 0$), there is no positive critical pressure, whereas for $k = -1$, one can obtain a real positive critical pressure when $\frac{s(n+1)-1}{s(n-3)+1} \in \mathbb{N}$. In the case of spherical horizon ($k = 1$), the sign of $P_{critical}/_{max}$ is depending on the values of nonlinearity, dimensionality and electric charge. One may find that for sufficiently large values of q , s and n , the second term will be less than one and one can obtain a positive critical pressure, while for usual values of the mentioned parameter, $P_{critical}/_{max}$ can be negative and one concludes there is no critical behavior. In order to show the effects of different parameters on the critical behavior of system, we plot various $P - r_+$ and $P - T$ diagrams (Figs. 7–10).

Evidently, critical pressure is a decreasing function of the electric charge while its corresponding critical horizon radius is an increasing function of this parameter (left panel of Fig. 7). As for the effects of dimensionality, one can see that both critical horizon radius and pressure are increasing functions of this parameter (left panel of Fig. 8). The effects of nonlinearity parameter should be separated into two branches; for $0.5 < s < 1$, critical pressure is a decreasing function of s , while the corresponding critical horizon is an increasing function of it (left panel of Fig. 9). On the contrary, for $1 < s$, critical pressure is an increasing function of the nonlinearity parameter whereas its critical horizon radius is a decreasing function of it (left panel of Fig. 10). These opposite behaviors for these two branches, highlight the differences between this nonlinear electromagnetic field and Born-Infeld like in which the effects of nonlinearity parameter are fixed.

As for CIM case, evidently, critical temperature and pressure are decreasing functions of the electric charge, while the critical horizon radius is an increasing function of it (Fig. 11). The effects of dimensionality is opposite of

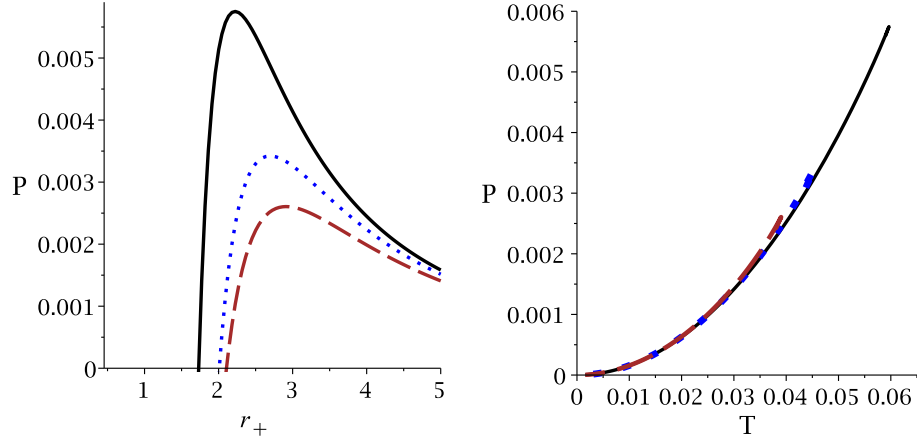


FIG. 9: Left panel: P versus r_+ diagrams; Right panel: P versus T diagrams. for $k = 1$, $n = 3$ and $q = 1.1$; $s = 0.7$ (continues line), $s = 0.8$ (dashed line) and $s = 0.9$ (dotted line).

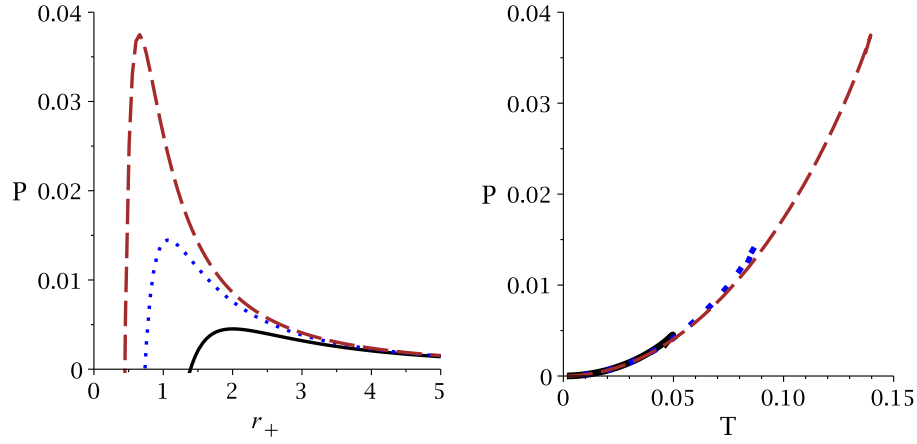


FIG. 10: Left panel: P versus r_+ diagrams; Right panel: P versus T diagrams. for $k = 1$, $n = 3$ and $q = 1.1$; $s = 1.1$ (continues line), $s = 1.2$ (dashed line) and $s = 1.25$ (dotted line).

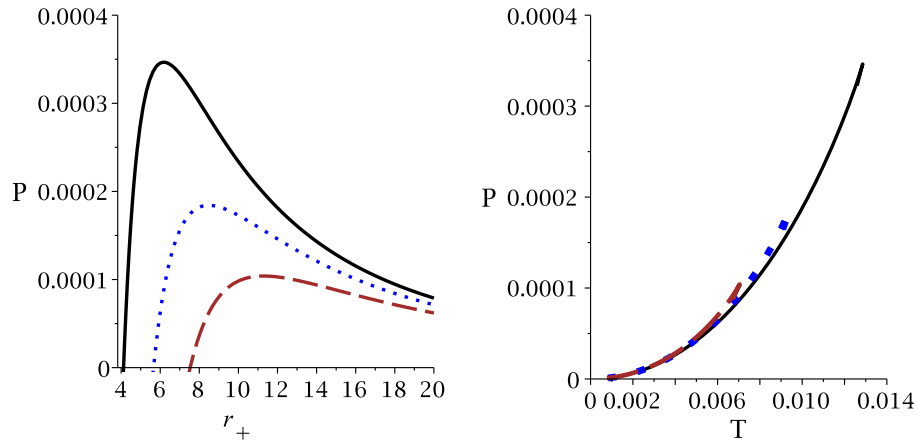


FIG. 11: Left panel: P versus r_+ diagrams; Right panel: P versus T diagrams. for $k = 1$, $n = 3$ and $l = 1$; $q = 0.9$ (continues line), $q = 1$ (dashed line) and $q = 1.1$ (dotted line).

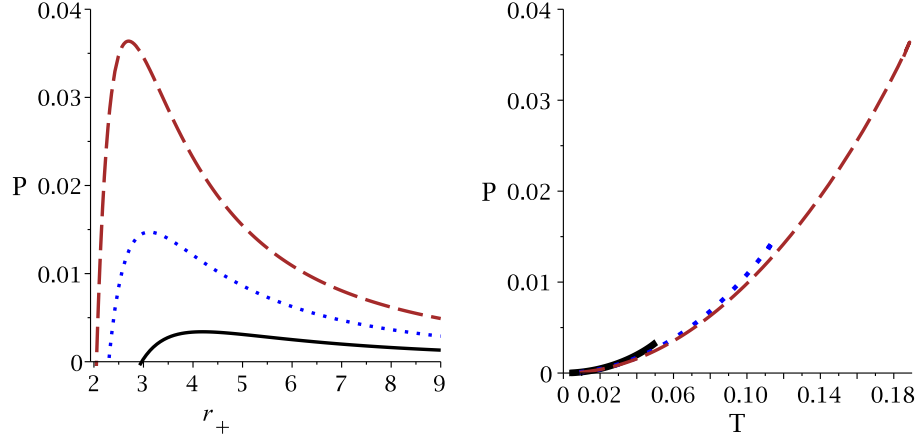


FIG. 12: Left panel: P versus r_+ diagrams; Right panel: P versus T diagrams. for $k = 1$, $l = 1$ and $q = 1.1$; $n = 4$ (continues line), $n = 5$ (dashed line) and $n = 6$ (dotted line).

the variation of electric charge. Meaning that, the critical pressure and temperature are increasing functions of the dimensionality while the critical horizon radius is a decreasing function of this parameter (Fig. 12).

E. van der Waals properties

In this subsection, we will investigate some van der Waals like properties of the solutions in the extended phase space. The presence of pressure in thermodynamical quantities and having equation of state at hand, one is able to extract volume expansion coefficient, speed of sound and isothermal compressibility coefficient of these black holes.

The volume expansion coefficient is calculated at constant pressure and it represents changes in volume of the black holes which takes place due to heat transferring. The volume expansion coefficients for two cases of this paper are given by [108]

$$\alpha = \frac{1}{V} \left(\frac{\partial V}{\partial T} \right)_P = \begin{cases} \frac{4\pi n(n-1) r_+^{n+1}}{16\pi P r_+^{n+2} - k(n-1)(n-2)r_+^n + q^n 2^{n/2} (n(n-2)+1)r_+^2}, & s = \frac{n}{2} \\ \frac{4\pi n(n-1) r_+^{\frac{2s(n-2)+1}{2s-1}}}{16\pi P r_+^{\frac{2s(n-1)}{2s-1}} - k(n-1)(n-2)r_+^{\frac{2(s(n-3)+1)}{2s-1}} + \frac{(q^2(n-1)(n-2s)^2)^s (2s(n-2)+1)}{(n-2)^s (2s-1)^{2s}}}, & \text{otherwise} \end{cases}. \quad (29)$$

The isothermal compressibility coefficient is calculated at constant temperature and it represents the corresponding effects of variation in volume with respect to change in pressure. Here, one can obtain this coefficient as [108]

$$\kappa_T = -\frac{1}{V} \left(\frac{\partial V}{\partial P} \right)_T = \begin{cases} \frac{16\pi n r_+^{n+2}}{16\pi P r_+^{n+2} - k(n-1)(n-2)r_+^n + 2^{n/2} q^n (n(n-2)+1)r_+^2}, & s = \frac{n}{2} \\ \frac{16\pi n r_+^{\frac{2s(n-1)}{2s-1}}}{16\pi P r_+^{\frac{2s(n-1)}{2s-1}} - k(n-1)(n-2)r_+^{\frac{2(s(n-3)+1)}{2s-1}} + \frac{(q^2(n-1)(n-2s)^2)^s (2s(n-2)+1)}{(n-2)^s (2s-1)^{2s}}}, & \text{otherwise} \end{cases} \quad (30)$$

where we have employed

$$\left(\frac{\partial V}{\partial P} \right)_T \left(\frac{\partial P}{\partial T} \right)_V \left(\frac{\partial T}{\partial V} \right)_P = -1. \quad (31)$$

The speed of sound in black holes does not carries its usual meaning. Here, while the area of black holes is fixed, the speed of sound indicates a breathing mode for variation of the volume with pressure. For obtaining speed of sound,

one should first calculate the homogenous density which for two cases here, can be written as [109, 110]

$$\rho = \frac{M}{V} = \begin{cases} P + \frac{kn(n-1)}{16\pi r_+^2} - \frac{2^{n/2} q^n n(n-1) \ln\left(\frac{r_+}{l}\right)}{16\pi r_+^n}, & s = \frac{n}{2} \\ P + \frac{n(n-1)k}{16\pi r_+^2} + \frac{n(q^2(n-1)(n-2s)^2)^s (2s-1)^2}{16\pi(n-2)^s (2s-1)^{2s} (n-2s)r_+^{\frac{2s(n-1)+1}{2s-1}}}, & \text{otherwise} \end{cases}. \quad (32)$$

Now, by employing the method of Refs. [109, 110], we obtain

$$c_s^{-2} = \frac{\partial \rho}{\partial P} = 1 + \rho \kappa, \quad (33)$$

in which confirms that speed of sound for these black holes is in the valid region of $0 \leq c_s^2 \leq 1$.

Obtained volume expansion and isothermal compressibility coefficients share identical denominator. Therefore, their divergencies are matched. Here, we focus only on the volume expansion coefficient. In order to have a better picture regarding the meaning of divergencies and the sign of this quantity, we have plotted its diagrams with the heat capacity and Ricci scalar of HPEM metric in Figs. 1-5 (dashed-dotted lines).

First of all, as one can see, the divergencies of volume expansion coefficient and heat capacity are matched. This shows that phase transition points that are observed in the heat capacity could be detected by studying the divergencies of volume expansion coefficient as well. In other words, the divergencies of volume expansion coefficient mark points in which black holes go under second order phase transition. In the absence of divergency for the volume expansion coefficient, this quantity is positive valued. On the contrary, when this quantity acquires divergences, its sign changes at the divergence points. By taking a closer look at the phase diagrams, one can see that the regions in which black holes are stable, the volume expansion coefficient is positive valued. On the contrary, in the unstable regions (negative heat capacity), the sign of volume expansion coefficient is negative. Here, we see that the sign of heat capacity and the volume expansion coefficient are identical in physical regions (positive) while in the non-physical region (negative temperature), there is a differences between the sign of these two quantities. It is worthwhile to mention that for the negative volume expansion coefficient, speed of sound will exceed the speed of light which is not physically acceptable. This indicates that between two divergencies, no physical black hole solutions exist.

Evidently, different approaches toward studying critical behavior of the black holes yield consisting results regarding the number and places of phase transition points. But, as one can see, each one of the phase diagrams carries specific information regarding thermodynamical structure and properties of the black holes which could not be acquired by other phase diagrams. Therefore, for having a better and more complete picture regrading thermodynamical behaviour/structure/properties of black holes, studying different phase diagrams is necessary and crucial.

IV. CONCLUSION

In this paper, we have investigated thermodynamical structure of Einstein black holes in the presence of PMI nonlinear electromagnetic field through new techniques.

It was shown that the behavior of temperature and stability conditions for these black holes were functions of different parameters describing the phase structure of these black. Interestingly, it was shown that the nonlinearity of system and the electric charge are two opposing factors in phase structure of these black holes. This behavior precisely highlights the differences between this theory of nonlinear electromagnetic field and Born-Infeld like theories. In Born-Infeld theories, the effects of both nonlinearity parameter and electric charge are similar. Here, we see that in PMI theory, these effects are in opposite of each other.

Next, geometrical thermodynamics was employed to investigate thermodynamical behavior of these black holes. It was pointed out that employing the Ruppeiner, Weinhold and Quevedo metrics will lead to anomaly while using HPEM metric, one obtains consistent results. The properties of HPEM metric around bound and phase transition points were highlighted as well. It was shown that (un)changing the sign of thermodynamical Ricci scalar around divergence points helps one to distinguish bound point from phase transition ones.

In addition, the proportionality between cosmological constant and thermodynamical pressure in denominator of the heat capacity was employed to extract a relation for thermodynamical pressure (independent of equation of state). Using the new pressure relation, it was possible to study the critical behavior of black hole system. Besides, the effects of different parameters on the critical pressure and horizon radius were investigated and it was shown that positivity of critical pressure and horizon radius were subjects to the choices of different parameters. In other words, it was possible to eliminate the existence of second order phase transition in phase space of these black holes by specific choices of different parameter.

Finally, we have conducted a study regarding thermodynamical properties of these black holes including volume expansion coefficient, speed of sound and isothermal compressibility coefficient. We have pointed out that divergencies of the volume expansion coefficient were matched with phase transition points in the heat capacity. This leads to a coincidence between divergencies of the Ricci scalar of HPEM and volume expansion coefficient. Furthermore, we showed that the sign of volume expansion coefficient were same as that of the heat capacity in physical regions ($T > 0$) while in the non-physical region ($T < 0$), these two signs were opposite.

The thermodynamical behavior that we observed here highly depends on choices of the nonlinearity parameter. In specific regions of the nonlinearity parameter, we observed a series of the effects which were modified in other regions for nonlinearity parameter. This characteristic behavior is not observed in Born-Infeld like family of the nonlinear electromagnetic fields. Meaning that the PMI theory not only differs from Born-Infeld like theories in form, but the characteristic behavior is different and only observed in this theory of the nonlinear electromagnetic field. These modifications in thermodynamical behavior of the black holes signal the fact that evolution of the black holes in this theory is different from other charged black holes. Therefore, the trace of these differences may be observable in properties such as quasi normal modes, gravitational waves and Hawking radiation and provide interesting case studies in other aspects of physics such as gauge/gravity duality.

Acknowledgments

We would like to thank the referees for the valuable comments. We also wish to thank Shiraz University Research Council. This work has been supported financially by the Research Institute for Astronomy and Astrophysics of Maragha, Iran.

-
- [1] B. P. Abbott et al., Phys. Rev. Lett. **116**, 061102 (2016).
 - [2] W. Heisenberg and H. Euler, Z. Phys. **98**, 714 (1936).
 - [3] H. H. Soleng, Phys. Rev. D **52**, 6178 (1995).
 - [4] H. Yajima and T. Tamaki, Phys. Rev. D **63**, 064007 (2001).
 - [5] D. H. Delphenich, [arXiv:hep-th/0309108].
 - [6] D. H. Delphenich, [arXiv:hep-th/0610088].
 - [7] I. Zh. Stefanov, S. S. Yazadjiev and M. D. Todorov, Mod. Phys. Lett. A **22**, 1217 (2007).
 - [8] L. Hollenstein and F. S. N. Lobo, Phys. Rev. D **78**, 124007 (2008).
 - [9] O. Miskovic and R. Olea, Phys. Rev. D **83**, 064017 (2011).
 - [10] M. Sharif and M. Azam, J. Phys. Soc. Jpn. **81**, 124006 (2012).
 - [11] J. Diaz-Alonso and D. Rubiera-Garcia, Gen. Relativ. Gravit. **45**, 1901 (2013).
 - [12] S. H. Hendi, Ann. Phys. **333**, 282 (2013).
 - [13] A. Sheykhi and S. Hajkhalili, Phys. Rev. D **89**, 104019 (2014).
 - [14] S. H. Mazharimousavi, M. Halilsoy and O. Gurtug, Eur. Phys. J. C **74**, 2735 (2014).
 - [15] S. H. Hendi, Ann. Phys. **346**, 42 (2014).
 - [16] L. Balart and E. C. Vagenas, Phys. Rev. D **90**, 124045 (2014).
 - [17] S. H. Hendi, Adv. High Energy Phys. **2014**, 697914 (2014).
 - [18] S. I. Kruglov, Phys. Rev. D **92**, 123523 (2015).
 - [19] I. Dymnikova and E. Galaktionov, Class. Quantum Gravit. **32**, 165015 (2015).
 - [20] S. H. Hendi, B. Eslam Panah and S. Panahiyan, Phys. Rev. D **91**, 084031 (2015).
 - [21] S. H. Hendi, S. Panahiyan and B. Eslam Panah, Eur. Phys. J. C **75**, 296 (2015).
 - [22] E. L. B. Junior, M. E. Rodrigues and M. J. S. Houndjo, JCAP **10**, 060 (2015).
 - [23] S. H. Hendi, B. Eslam Panah, M. Momennia and S. Panahiyan, Eur. Phys. J. C **75**, 457 (2015).
 - [24] A. Sepehri and A. F. Ali, [arXiv:1602.06210].
 - [25] S. H. Hendi, M. R. Hadizadeh and R. Katebi, Iran. J. Sci. Technol. Trans. Sci. (to be published: DOI 10.1007/s40995-016-0060-5).
 - [26] M. Hassaine and C. Martinez, Class. Quantum Gravit. **25**, 195023 (2008).
 - [27] H. Maeda, M. Hassaine and C. Martinez, Phys. Rev. D **79**, 044012 (2009).
 - [28] S. H. Hendi, Phys. Lett. B **678**, 438 (2009).
 - [29] S. H. Hendi, Class. Quantum Gravit. **26**, 225014 (2009).
 - [30] S. H. Hendi, B. Eslam Panah and R. Safari, Int. J. Mod. Phys. D **23**, 1450088 (2014).
 - [31] S. H. Hendi and B. Eslam Panah, Phys. Lett. B **684**, 77 (2010).
 - [32] O. Gurtug, S. Habib Mazharimousavi and M. Halilsoy, Phys. Rev. D **85**, 104004 (2012).
 - [33] S. H. Hendi, S. Panahiyan and E. Mahmoudi, Eur. Phys. J. C **74**, 3079 (2014).
 - [34] M. Zhang, Z. Y. Yang, D. C. Zou, W. Xu and R. H. Yue, Gen. Relativ. Gravit. **47**, 14 (2015).

- [35] M. Kord Zangeneh, A. Sheykhi and M. H. Dehghani, *Eur. Phys. J. C* **75**, 497 (2015).
- [36] J. X. Mo, G. Q. Li and X. B. Xu, *Phys. Rev. D* **93**, 084041 (2016).
- [37] M. Hassaine and C. Martinez, *Phys. Rev. D* **75**, 027502 (2007).
- [38] S. H. Hendi and H. R. Rastegar-Sedehi, *Gen. Relativ. Gravit.* **41**, 1355 (2009).
- [39] S. H. Hendi, *Phys. Lett. B* **677**, 123 (2009).
- [40] D. Roychowdhury, *Phys. Lett. B* **718**, 1089 (2013).
- [41] S. Hawking and D. N. Page, *Commun. Math. Phys.* **87**, 577 (1983).
- [42] R. G. Cai, S. P. Kim and B. Wang, *Phys. Rev. D* **76**, 024011 (2007).
- [43] R. G. Cai, L. M. Cao and Y. W. Sun, *JHEP* **11**, 039 (2007).
- [44] M. Eune, W. Kim and S. H. Yi, *JHEP* **03**, 020 (2013).
- [45] P. C. W. Davies, *Proc. Roy. Soc. Lond. A* **353**, 499 (1977).
- [46] G. Gibbons, R. Kallosh and B. Kol, *Phys. Rev. Lett.* **77**, 4992 (1996).
- [47] J. D. E. Creighton and R. B. Mann, *Phys. Rev. D* **52**, 4569 (1995).
- [48] B. P. Dolan, *Class. Quantum Gravit.* **28**, 125020 (2011).
- [49] B. P. Dolan, *Class. Quantum Gravit.* **28**, 235017 (2011).
- [50] R. Banerjee and D. Roychowdhury, *Phys. Rev. D* **85**, 044040 (2012).
- [51] R. Banerjee and D. Roychowdhury, *Phys. Rev. D* **85**, 104043 (2012).
- [52] D. Kubiznak and R. B. Mann, *JHEP* **07**, 033 (2012).
- [53] R. G. Cai, L. M. Cao, L. Li and R. Q. Yang, *JHEP* **09**, 005 (2013).
- [54] M. B. Jahani Poshteh, B. Mirza and Z. Sherkatghanad, *Phys. Rev. D* **88**, 024005 (2013).
- [55] S. Chen, X. Liu and C. Liu, *Chin. Phys. Lett.* **30**, 060401 (2013).
- [56] S. H. Hendi and M. H. Vahidinia, *Phys. Rev. D* **88**, 084045 (2013).
- [57] J. X. Mo and W. B. Liu, *Eur. Phys. J. C* **74**, 2836 (2014).
- [58] D. C. Zou, S. J. Zhang and B. Wang, *Phys. Rev. D* **89**, 044002 (2014).
- [59] W. Xu and L. Zhao, *Phys. Lett. B* **736**, 214 (2014).
- [60] A. M. Frassino, D. Kubiznak, R. B. Mann and F. Simovic, *JHEP* **09**, 214 (2014).
- [61] J. Xu, L. M. Cao and Y. P. Hu, *Phys. Rev. D* **91**, 124033 (2015).
- [62] S. H. Hendi, S. Panahiyan and M. Momennia, *Int. J. Mod. Phys. D* **25**, 1650063 (2016).
- [63] S. H. Hendi, S. Panahiyan and B. Eslam Panah, *Prog. Theor. Exp. Phys.* **2015**, 103E01 (2015).
- [64] S. H. Hendi, B. Eslam Panah and S. Panahiyan, *JHEP* **11**, 157 (2015).
- [65] S. H. Hendi, B. Eslam Panah and S. Panahiyan, *Class. Quantum Grav.* **33**, 235007 (2016).
- [66] R. Banerjee, B. R. Majhi and S. Samanta, [arXiv:1611.06701].
- [67] A. Mandal, S. Samanta and B. R. Majhi, *Phys. Rev. D* **94**, 064069 (2016).
- [68] B. R. Majhi, S. Samanta, [arXiv:1609.06224].
- [69] S. H. Hendi, R. B. Mann, S. Panahiyan and B. Eslam Panah, *Phys. Rev. D* **95**, 021501(R) (2017).
- [70] C. V. Johnson, *Class. Quantum Gravit.* **31**, 205002 (2014).
- [71] B. P. Dolan, *JHEP* **10**, 179 (2014).
- [72] E. Caceres, P. H. Nguyen and J. F. Pedrazab, *JHEP* **09**, 184 (2015).
- [73] B. P. Dolan, *Mod. Phys. Lett. A* **30**, 1540002 (2015).
- [74] S. H. Hendi, S. Panahiyan and R. Mamasani, *Gen. Relativ. Gravit.* **47**, 91 (2015).
- [75] S. H. Hendi, S. Panahiyan and B. Eslam Panah, *Int. J. Mod. Phys. D* **25**, 1650010 (2016).
- [76] F. Weinhold, *J. Chem. Phys.* **63**, 2479 (1975).
- [77] F. Weinhold, *J. Chem. Phys.* **63**, 2484 (1975).
- [78] G. Ruppeiner, *Phys. Rev. A* **20**, 1608 (1979).
- [79] G. Ruppeiner, *Rev. Mod. Phys.* **67**, 605 (1995).
- [80] P. Salamon, J. Nulton and E. Ihrig, *J. Chem. Phys.* **80**, 436 (1984).
- [81] H. Quevedo, *J. Math. Phys.* **48**, 013506 (2007).
- [82] H. Quevedo and A. Sanchez, *JHEP* **09**, 034 (2008).
- [83] S. H. Hendi, S. Panahiyan, B. Eslam Panah and M. Momennia, *Eur. Phys. J. C* **75**, 507 (2015).
- [84] S. H. Hendi, S. Panahiyan and B. Eslam Panah, *Adv. High Energy Phys.* **2015**, 743086 (2015).
- [85] S. H. Hendi, A. Sheykhi, S. Panahiyan and B. Eslam Panah, *Phys. Rev. D* **92**, 064028 (2015).
- [86] S. H. Hendi, B. Eslam Panah and S. Panahiyan, *JHEP* **05**, 029 (2016).
- [87] S. A. Hosseini Mansoori and B. Mirza, *Eur. Phys. J. C* **74**, 2681 (2014).
- [88] S. A. Hosseini Mansoori, B. Mirza and M. Fazel, *JHEP* **04**, 115 (2015).
- [89] S. A. Hosseini Mansoori, B. Mirza and E. Sharifian, *Phys. Lett. B* **759**, 298 (2016).
- [90] R. Banerjee, S. Ghosh and D. Roychowdhury, *Phys. Lett. B* **696**, 156 (2011).
- [91] K. C. K. Chan, J. H. Horne and R. B. Mann, *Nucl. Phys. B* **447**, 441 (1995).
- [92] G. Ruppeiner, *Springer Proc. Phys.* **153**, 179 (2014).
- [93] H. Quevedo, *Gen. Relativ. Gravit.* **40**, 971 (2008).
- [94] D. Pavon and J. M. Rubi, *Gen. Relativ. Gravit.* **18**, 1245 (1986).
- [95] J. Maddox, *Nature* **365**, 103 (1993).
- [96] C. Tsallis, *Chaos, Soliton and Fractals* **12**, 371 (2002).
- [97] J. Oppenheim, *Phys. Rev. E* **68**, 016108 (2003).
- [98] C. Tsallis and L. J. L. Cirto, *Eur. Phys. J. C* **73**, 2487 (2013).

- [99] S. Carlip, [arXiv:1410.1486].
- [100] Y. C. Ong, JCAP **04**, 003 (2015).
- [101] H. Quevedo, M. N. Quevedo , A. Sanchez and S. Taj, Phys. Scripta **8**, 084007 (2014).
- [102] A. Bravetti, C. S. L. Monsalvo, F. Nettel, and H. Quevedo, J. Math. Phys. **54**, 033513 (2013).
- [103] S. H. Hendi, B. Eslam Panah and S. Panahiyan, JHEP **11**, 157 (2015).
- [104] S. H. Hendi, S. Panahiyan and B. Eslam Panah, JHEP **01**, 129 (2016).
- [105] H. Quevedo, M.N. Quevedo and A. Sánchez, Phys. Rev. D **94**, 024057 (2016).
- [106] S. H. Hendi, N. Riazi and S. Panahiyan, [arXiv:1610.01505].
- [107] S. H. Hendi, S. Panahiyan, S. Upadhyay and B. Eslam Panah, [arXiv:1611.02937].
- [108] J. X. Mo and W. B. Liu, Phys. Rev. D **89**, 084057 (2014)
- [109] B. P. Dolan, Phys. Rev. D **84**, 127503 (2011).
- [110] B. P. Dolan, Class. Quantum Gravit. **31**, 035022 (2014).